GEOPHYSICAL RESEARCH LETTERS, VOL. 19, NUMBER 24, PAGES 2409-2412, DECEMBER 24, 1992

FIRST OBSERVATIONS OF PRECIPITATION WITH A SPATIAL INTERFEROMETER

P.B. Chilson, R.D. Palmer[1], M.F. Larsen, C.W. Ulbrich
Department of Physics and Astronomy, Clemson University

S. Fukao, M. Yamamoto, T. Tsuda and S. Kato
Radio Atmospheric Science Center, Kyoto University

Abstract. This paper presents the initial results of a study of precipitation using spatial interferometry (SI) at the MU radar in Japan. On April 30, 1992, data were collected using the VHF Doppler radar at the facility during the passage of a frontal system. A linear variation in the phase was identified in the cross-spectra of the returned signal in the Doppler velocity ranges corresponding to contributions from both precipitation and refractive index irregularities of the turbulent air. The portions of the spectra which are attributed to precipitation are broadened by the range of particle sizes and the presence of turbulence. This leads to a larger underestimation in the slope of the phase than would be attributed to turbulent fading alone. The results present the first radar interferometry study of precipitation.

1 Introduction

The effectiveness of using spatial interferometry (SI) for investigating atmospheric dynamics has been well established [*e.g., Meek and Manson*, 1987; *Larsen and Röttger*, 1991]. Although the technique was first devised for studying the inclination of the geomagnetic field [*Woodman*, 1971], the method was quickly shown to be useful in observing distributed scatters such as refractive index irregularities in the lower atmosphere. By analyzing the phase of the returned signal, SI can be used to estimate the three dimensional wind within the sampling volume. The technique has been described by *Palmer et al.* [1991], *Van Baelen and Richmond* [1991], and *Larsen et al.* [1992] where it is shown to be the Fourier transform equivalent of the spaced antenna (SA) technique. The estimated SI wind vector is equivalent to the so-called SA apparent velocity and a scheme for obtaining the true velocity from the frequency domain has been derived [*Briggs and Vincent*, 1992; *Sheppard and Larsen*, 1992] using a Fourier transform equivalent of the full correlation analysis (FCA) called full spectral analysis (FSA).

The potential advantage of using SI for precipitation studies is that the fine scale structure of the particles within the angular spread of the radar beam can be determined. Also, as will be shown later, the phase information may be useful in estimating the effect of turbulent broadening. To date, no observations of precipitation have been made using SI. Indeed, it has been unknown whether SI would work in such an analysis. The spectra formed by the backscattered signal from turbulent variations in the refractive index usually approximate a Gaussian distribution in velocity space [*Woodman*, 1985]. The strength of the signal, the mean Doppler velocity and the estimate of turbulence intensity can be determined from the spectral moments of the Doppler spectra. In a non-turbulent environment with no wind, spectra resulting from scatter off a collection of precipitation particles follow a distribution which varies as a function of the particle sizes when observed by a vertically pointing Doppler radar. The form of the precipitation spectrum in velocity space is then dependant on the fall speeds of the particles as a function of diameter. Such an environment is rarely observed in reality and the effects of turbulence and wind on the precipitation spectra will be discussed later. Other factors affecting the spectra such as wind shear, beam broadening and spatial averaging will be addressed in future work.

2 Spatial Interferometry

Following the discussion by *Larsen et al.* [1992], the relevant equations for SI will be outlined here. If two spatially separated receiving antennas, i and j, detect the returned signal from a common scatterer or scattering medium, the difference in phase measured by the two receivers will be related to the radar wavenumber k, their separation d_{ij} and the zenith angle δ through

$$\phi_{ij} = k d_{ij} \sin\delta. \tag{1}$$

The angle δ is measured within the vertical plane containing the two receivers. In the case of a vertically pointing radar, the range of the sampled zenith angles is determined by the width of the transmitted beam and the reflectivity field within the resolution volume. If the scatterers are moving horizontally through the sampling volume with a uniform speed and the direction of the wind is parallel to a baseline of the receiving antennas, then the detected radial velocity will vary from $-v\sin\delta$ to $+v\sin\delta$, where v is the actual horizontal wind speed. In this analysis, the common assumption has been made that the Taylor hypothesis is valid.

By finding the Fourier transforms $F_i(\omega)$ and $F_j(\omega)$ obtained from two spatially separated receiving arrays i and j, the cross-spectrum can be obtained

$$C_{ij}(\omega) = F_i(\omega)F_j^*(\omega) = A_i(\omega)A_j(\omega)e^{i[\phi_i(\omega)-\phi_j(\omega)]} \tag{2}$$

[1]Now with the Department of Electrical Engineering, University of Nebraska-Lincoln, Lincoln, Nebraska 68588-0511.

Paper number 92GL02629
0094-8534/92/92GL-02629$03.00

where ω is the frequency, $A_i(\omega)$ and $A_j(\omega)$ are the amplitudes and ϕ_i and ϕ_j are the phases of the Fourier transforms. The * denotes the complex conjugate. The amplitude of the cross-spectrum should be approximately the same as that of the auto-spectrum since $F_i(\omega)$ and $F_j(\omega)$ are obtained from essentially the same scattering volume. The Doppler sorting process leads to a linear variation in the phase of the cross-spectrum.

Larsen et al. [1992] derived the equations relating the wind velocity to the slope and intercept of the phase variation in the cross-spectrum. If the wind vector is decomposed into a horizontal component, v_h, and a vertical component, w, then the radial Doppler velocity v_r can be expressed as

$$v_r = v_h \frac{sin\delta}{cos(\alpha_{ij} - \theta)} + w \tag{3}$$

where α_{ij} and θ are the azimuth angles for the baseline between two receiving antennas and the wind vector, respectively. By using Eqs. (1) and (3) and solving for ϕ_{ij} one finds

$$\phi_{ij} = \frac{kd_{ij}cos(\alpha_{ij} - \theta)}{v_h}(v_r - w) \tag{4}$$

i.e., a linear equation for the slope of the line defining the variation of the phase in the cross-spectrum. In obtaining Eq. (4) δ has been assumed to be small, allowing the approximation to be made that $cos\delta \sim 1$ and $sin\delta \sim tan\delta$. Substituting the slopes and intercepts found from the cross-spectra of two pairs of baselines along with their azimuth angles, the magnitude and direction of the apparent wind can be estimated.

The velocities given by Eq. (4) are the apparent velocities in that turbulent fading has not been taken into account. Another assumption is that w is not affected by aspect sensitivity, i.e., the scattering is isotropic within the sampling volume. Any layering of the atmosphere would give rise to specular backscatter at VHF frequencies [*e.g. Tsuda et al.*, 1986], leading in turn to an erroneous estimation of the vertical wind if the layers are inclined with respect to horizontal. However, *Larsen et al.* [1992] have shown that the effects of aspect sensitivity can also be handled with an SI analysis only slightly more complicated than the one presented here. The estimation of the horizontal wind, and thus the slope of the cross-spectral phase, is not affected by the layering. Since the primary concern of this work has been to show the variations in the phase of the cross-spectrum seen in the signal associated with the precipitation, no efforts have been made to correct for the effect of specularity in the present analysis.

3 Description of the Experiment

The data presented in this paper were taken on April 30, 1992, at the MU radar located at Shigaraki, Japan (34.85° N, 136.10° E). A front which passed the radar site resulted in heavy, stratiform rain. The radar's entire phased array antenna was used for transmission, but was partitioned into three separate subarrays in a triangular configuration for reception. The operating frequency of the MU radar is 46.5 MHz giving a wavelength of 6.45 m. A pulse width of 1 μs was used during transmission giving a height resolution of 150 m. Height coverage extended from 1.8 km to 9.6 km ASL. The inter-pulse period (IPP) was 400 μs and 256 samples were coherently integrated, resulting in a sampling period of 0.1024 s and a Nyquist velocity of ± 16 ms^{-1}. The data presented in this work were obtained using 16 incoherent integrations which translates into approximately 7 minutes of real time data. Brief gaps in the data for data storage led to an actual dwell time nearer to 8 minutes. A long integration time was chosen to facilitate the phase analysis of the precipitation signal, which will be discussed below.

An example of the auto-spectra resulting from the 256-pt FFT is presented as a function of height in Figure 1a. The spectra are shown using a linear power spectral density scale and they have been normalized to the peak at each altitude. The corresponding combined power from the turbulence and precipitation is shown in Figure 2b. The radar has not been calibrated, so the power profile indicates only the relative change in the backscattered signal. An interesting feature of the profile is the abrupt increase in echo power at 3 km. In addition, below 3 km, a bimodal pattern is observed in the spectra, and the two peaks are seen to separate in velocity. The peak in a particular spectrum associated with a more negative velocity (towards the radar) is attributed to the falling precipitation and will be referred to as the precipitation peak. The other peak is attributed to the turbulent variations of the refractive index and will be referred to as the turbulence peak. The height where the two spectral peaks begin to separate and also where the enhanced reflectivities occur is indicative of the location of the melting layer or bright band [*Battan*, 1973]. In the transition region in which the spectra become bimodal (3.0 – 3.6 km), the precipitation peak is much larger than the turbulence peak causing the latter to be lost in the spectral noise. Although the presence of a bright band at

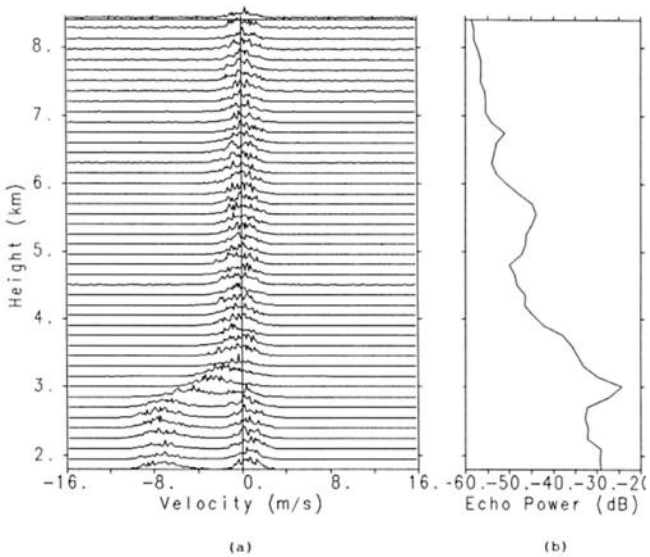

Fig. 1. (a) Doppler spectra obtained at 0530 LT plotted over the range of sampled heights. The spectra, which have been normalized to the peak power at each height, are displayed using a linear scale. (b) The corresponding relative echo power.

VHF is not well documented, a similar pattern has been seen at 53.5 MHz by *Yoe* [1990].

4 Analysis and Results

As shown above, the SI analysis involves using the phase of the cross-spectrum. When examining the phase, it is important to choose a spectral window broad enough to provide adequate data for the statistics without including the noise. For a given spectral peak, its amplitude in the cross-spectrum relative to its amplitude in the auto-spectrum is a measure of the coherence. Therefore only regions of the cross-spectrum where the relative amplitudes are large should exhibit consistency in the phase. The method chosen for this analysis was to fit one or two Gaussian distributions to the spectrum and use the fitted parameters as an estimate of the widths. All data within $\pm 2\sigma$ of the peak or peaks of the distribution were used in the phase analysis. This also provided a method of isolating the two peaks in those cases where the spectrum was bimodal. Although the turbulence peak is well approximated by a Gaussian, the normalized precipitation spectrum observed with a vertically pointing radar is better represented by

$$S_p(v_r) = \frac{1}{Z} D^6 N(D) \frac{dD}{dv_r} \tag{5}$$

where Z is the radar reflectivity factor, $N(D)$ is a distribution function of the diameters D of the precipitation particles, and v_r is their fall speed [*Battan*, 1973]. Eq. (5) assumes the particles are falling through a quiescent atmosphere in the absence of any turbulence or vertical wind. The actual observed precipitation peak is a convolution of Eq. (5) with the turbulence portion of the spectrum [*Wagasuki et al.*, 1987; Gossard *et al.*, 1990]. The resulting bimodal spectrum takes the form

$$S_o(v_r) = P_p S_p(v_r - w) \otimes S_t(v_r) + P_t S_t(v_r - w) \tag{6}$$

where P_p and P_t are the spectral powers from the precipitation and turbulence contributions, respectively, and $S_t(v_r)$ is the normalized Gaussian spectrum for the turbulence. The convolution operator is indicated by $\otimes$. Since the distribution of the precipitation particles is convolved with a Gaussian function, the precipitation peak can be fit sufficiently well to a Gaussian for the purpose of separating the two peaks and establishing an estimate of its width.

Having defined the spectral window, a line was fit to the phase as a function of velocity. As can be seen in Figure 2, a linear variation of the slope can be identified separately for both the contributions from turbulent variations in the refractive index and precipitation. The cross-spectra obtained for all three receiver combinations at a height of 2.1 km are shown for comparison. As is true for the winds, the goodness of fit of the phase to a linear function is most pronounced when the baseline is parallel to the wind vector, where spatial decorrelation is minimal. Calculations using the phase corresponding to the turbulence show the winds to be southerly at this altitude. Since the 2–3 baseline is almost perpendicular to the wind vector (Figure 2c), the phase shows a small slope. As was mentioned earlier, near the melting layer, the precipitation signal may dominate the spectrum making the signal from the turbulent

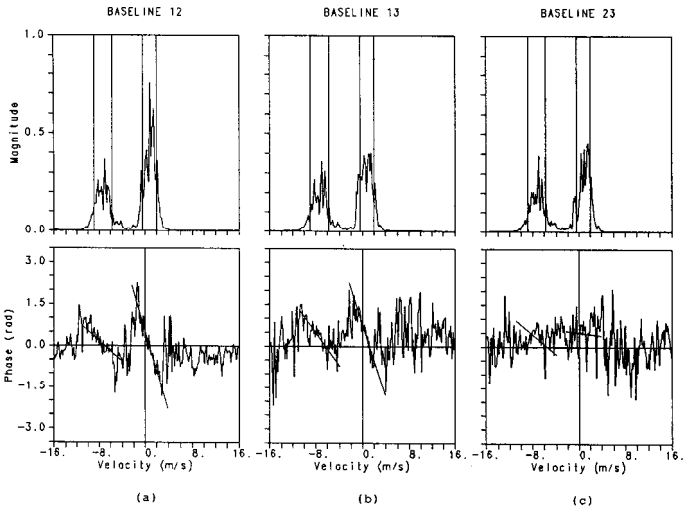

Fig. 2. An example of the cross-spectra for data obtained at 2.1 km. This corresponds to the data shown in Fig. 2. The magnitude and phase of the cross-spectra are shown in the upper and lower rows, respectively. Vertical lines have been included to indicate the range of data used to find the slope of the displayed fits. The cross-spectra obtained from receiver pairs 1–2, 1–3 and 2–3 are shown in (a), (b) and (c), respectively.

air difficult to resolve in spectral amplitude. Although the echo power from the turbulence is significantly less than that of the precipitation, in many cases the phase variations from both returns can still be detected.

Since no correction has been made in this analysis for the effects of turbulent fading, the slopes shown in Figure 2 are underestimated, i.e., the corresponding horizontal wind magnitude will be overestimated. Furthermore, it can be seen that the slopes of the phase from the precipitation return have still smaller values than those obtained from the turbulence signals. The slope is a measure of the apparent horizontal winds and the quotient of slope and intercept for the fitted line is a measure of the vertical wind if there are no aspect sensitivity effects [*Palmer et al.*, 1991]. The observed Doppler velocities in the precipitation portion of the spectrum represent not only the particle fall speeds, but turbulent broadening and beam broadening as well. Under the assumption that a collection of precipitation particles of similar dimension are carried along by the horizontal wind in the absence of turbulence and beam effects, the slopes in the phase from the rain and the wind should be approximately the same. The primary difference in the two would be in the intercepts which are affected by the magnitude of the vertical velocity. The data shown in Figure 2 clearly show this not to be the case. The phase slopes associated with the turbulence are more steeply inclined than those associated with the precipitation. The distribution of particle diameters also results in a broadening of the spectrum in velocity space. Any broadening of the spectrum in SI tends to decrease the lag time in the cross-correlation function, which is analogous to reducing the phase slope in the cross-spectrum.

In the present analysis, long integration times were chosen for the sake of showing the linear variation of the phase associated with the precipitation. This was done at the cost of losing the structure in the phase which is apparent

with less averaging. With a beamwidth of 3.6°, the sampling volume at 2.1 km has a diameter of approximately 132 m. The calculated SI apparent horizontal wind at 2.1 km is ~ 40 ms^{-1} indicating the radar is detecting a new volume of space every 3.3 seconds. The stratiform nature of both the wind and precipitation, however, makes the lengthy averaging of the data justifiable. A more detailed study of the data will require integration times of 30 seconds or less.

5 Conclusions

The data collected at the MU radar during the passage of a frontal system demonstrate the applicability of spatial interferometry to precipitation environments. A height profile of the spectra reveals a bimodal pattern developing near the melting layer and extending toward the surface. In those cases where both the precipitation and the winds are present in the Doppler spectrum and sufficiently well separated in velocity space, the slopes from each contribution can be identified. It is interesting to note that the variation in the phase can often be seen for a given spectral peak even when its amplitude is small.

Although precipitation particles should approximately follow the horizontal wind, the data show the slopes in the phase associated with the rain and the wind to be different. It is known that turbulence can decorrelate the signal recorded at two separate receiving antennas, thus reducing the slope in the phase. The turbulent fading can be removed [*Briggs and Vincent*, 1992] from the portion of the spectrum associated with the turbulent air to yield the true SI horizontal wind, but this has not been done in the present analysis. The precipitation peak of the spectrum should likewise be influenced by turbulent fading as seen in Eq. 6. This does not, however, account for the enhanced reduction of the slope. The further decorrelation of the signal might result from the distribution of the precipitation particles contained within the radar sampling volume. The spectral peak attributed to the precipitation is broadened in velocity space through the spread of the Doppler fall speeds. Any temporal decorrelation resulting from the velocity spreading would lead to an underestimation of the slope. A more thorough analysis of the data is needed to address this topic.

Acknowledgements. PBC and CWU were supported by the NSF under grant #ATM9003448, and RDP under NSF grants #ATM9121526, #ATM9006846 and #ATM9003448. MFL was supported by AFOSR grant AFOSR-91-0384. The MU radar belongs to and is operated by the Radio Atmospheric Center of Kyoto University, Japan.

References

Battan, L. J., *Radar Observations of the Atmosphere*, 324 pp., The University of Chicago Press, Chicago, 1973.

Briggs, B. and R. A. Vincent, Spaced-antenna analysis ir the frequency domain, *Radio Sci.*, *27*, 117–129, 1992.

Gossard, E. E., R. G. Strauch and R. R. Rogers, Eval uation of drop-size-distributions in liquid precipitatior observed by ground-based Doppler radar, *J. Atmos Oceanic Tech.*, *7*, 815–828, 1990

Larsen, M. F. and J. Röttger, VHF radar measurement: of refractivity layer tilt angles and associated vertical beam radial velocity corrections, *J. Atmos. Ocean Tech. 8*, 477–490, 1991.

Larsen, M. F., R. D. Palmer, S. Fukao, R. F. Wood man, M. Yamamoto, T. Tsuda and S. Kato, An anal ysis technique for deriving vector winds and in-beam incidence angles from interferometer measurements, *J Atmos. Ocean Tech.*, *9*, 3–14, 1992.

Meek, C. E. and A. H. Manson, Mesospheric motions ob served by simultaneous medium-frequency interferome ter and spaced antenna experiments, *J. Geophys. Res. 92*, 917–930, 1987.

Palmer, R. D., M. F. Larsen, R. F. Woodman, S. Fukao M. Yamamoto, T. Tsuda and S. Kato, VHF Radar In terferometry measurements of vertical velocities and th effect of tilted refractivity surfaces on standard Dopple measurements, *Radio Sci.*, *26*, 417–427, 1991.

Sheppard, E. L. and M. F. Larsen, Analysis of model simu lations of spaced antenna/radar interferometer measure ments, *Radio Sci.*, *27*, 759–768 1992.

Tsuda, T., T. Sato, K. Hirose, S. Fukao and S. Kato, MU radar observations of the aspect sensitivity of backscat tered VHF echo power in the troposphere and lowe stratosphere, *Radio Sci.*, *21*, 971–980, 1986.

Van Baelen, J. S. and A. D. Richmond, Radar interferom etry technique: Three-dimensional wind measuremen theory, *Radio Sci.*, *26*, 1209–1218, 1991.

Wagasuki, K., A. Mitzutani, S. Fukao and S. Kato, Fur ther discussions on deriving drop size distribution anc vertical air velocities from VHF Doppler radar spectra *J. Atmos. Oceanic Technol.*, *3*, 623–639 1987

Woodman, R., Inclination of the geomagnetic field mea sured by an incoherent scatter radar technique, *J. Geo phys. Res.*, *76*, 178–184, 1971.

Woodman, R., Spectral moment estimation in MST radars *Radio Sci.*, *20*, 1185–1195, 1985.

Yoe, J. G., *Analysis and comparison of several method for processing VHF Doppler radar wind profiler data ob tained during a mesoscale convective storm*, Ph.D. dis sertation, Clemson University, Clemson SC, 132pp.

P. B. Chilson, M. F. Larsen, R. D. Palmer, and C. W. Ul brich, Department of Physics and Astronomy, Clemsor University, Clemson, SC 29634.

S. Fukao, S. Kato, T. Tsuda, and M. Yamamoto, Radi Atmospheric Science Center, Kyoto University, Uji, Kyot 611, Japan.

(Received September 21, 1992;
Accepted October 14, 1992)